



The norepinephrine transporter gene modulates intrinsic brain activity, visual memory, and visual attention in children with attention-deficit/hyperactivity disorder

Chi-Yung Shang¹ · Hsiang-Yuan Lin¹ · Susan Shur-Fen Gau^{1,2}

Received: 11 October 2018 / Revised: 7 August 2019 / Accepted: 19 August 2019
© The Author(s), under exclusive licence to Springer Nature Limited 2019

Abstract

The norepinephrine transporter gene (*SLC6A2*) and deficits in visual memory and attention were associated with attention-deficit/hyperactivity disorder (ADHD). The present study aimed to examine whether the *SLC6A2* rs36011 (T)/rs1566652 (G) haplotype affected the intrinsic brain activity in children with ADHD and whether these gene-brain modulations were associated with visual memory and attention in this population. A total of 96 drug-naïve children with ADHD and 114 typically developing children (TDC) were recruited. We analyzed intrinsic brain activity with regional homogeneity (ReHo) and degree centrality (DC). Visual memory and visual attention were assessed by the delayed matching to sample (DMS) and rapid visual information processing (RVIP) tasks, respectively. The SNP genotyping of rs36011 and rs1566652 was performed. Children with ADHD showed lower ReHo and DC in the cuneus and lingual gyri than TDC. The TG haplotype was associated with significantly increased DC in the right precentral and postcentral gyri. Significant interactions of ADHD status and the TG haplotype were found in the right postcentral gyrus and superior parietal lobule for ReHo. For the ADHD-TG group, we found significant correlations of performance on the DMS and RVIP tasks with ReHo in bilateral precentral-postcentral gyri and the right postcentral gyrus-superior parietal lobule and DC in bilateral precentral-postcentral gyri. A novel gene-brain-behavior association was identified in which the intrinsic brain activity of the sensorimotor and dorsal attention networks was related to visual memory and visual attention in ADHD children with the *SLC6A2* rs36011 (T)/rs1566652 (G) haplotype.

Introduction

Attention-deficit/hyperactivity disorder (ADHD) is a common and highly heritable neuropsychiatric disorder in childhood, with compelling evidence of involving dopaminergic and noradrenergic neurotransmission systems [1]. One of the promising candidate genes for ADHD is the norepinephrine transporter gene, also known as solute

carrier family 6, member 2 (*SLC6A2*). *SLC6A2* is mapped on chromosome 16q12.2, consisting of 14 coding exons that span about 45 kb. It codes for the norepinephrine transporter (NET), which is crucial for the fine tuning of the dopaminergic [2] and noradrenergic [3] neurotransmission. Although allelic variations of *SLC6A2* may confer genetic risk for ADHD [4, 5], the exact mechanisms of the *SLC6A2* in the brain remain unclear [6].

Neuroimaging studies on the complex pathophysiology of ADHD implicate altered connections within and between major brain networks [7, 8]. In parallel to intrinsic functional connectivity network approaches, complementary local measurements, such as regional homogeneity (ReHo), characterizing the degree of local synchronization of intrinsic brain activity [9], and degree centrality (DC), measuring the local network connections [10], have also been applied to detect local abnormalities in ADHD. For example, previous studies demonstrate decreased ReHo in the medial prefrontal cortex [11], superior frontal gyri [12], precuneus [13], and cuneus [13], and increased ReHo in the

Supplementary information The online version of this article (<https://doi.org/10.1038/s41380-019-0545-7>) contains supplementary material, which is available to authorized users.

✉ Susan Shur-Fen Gau
gaushufe@ntu.edu.tw

¹ Department of Psychiatry, National Taiwan University Hospital, and College of Medicine, Taipei, Taiwan

² Graduate Institute of Brain and Mind Sciences, National Taiwan University, Taipei, Taiwan

sensorimotor region [12], paracentral lobule/postcentral [14], and lingual gyrus [15] in ADHD. In addition, increased DC in precuneus [16] and lingual gyrus [14], and decreased DC in insula [14] have been reported in ADHD.

Given that the pathway from gene to behavior is complex, imaging genetics studies have the potential to provide a more comprehensive understanding of the dynamic interplay of genes, brain and environment [17]. However, only limited studies have hitherto investigated the effects of *SLC6A2* on brain phenotypes in individuals with ADHD. Specifically, a previous study on the *SLC6A2* rs998424 and rs3785157 demonstrated that no genotype or genotype-by-diagnosis effects are observed in any of the measures of global and lobar brain volumes in children with ADHD [5]. A positron emission tomography study has reported significant *SLC6A2*-moderated correlations of hyperactivity/impulsivity symptoms with NET binding in the cerebellum in adults with ADHD [18]. A pharmacological neuroimaging study showed increased regional blood perfusion in the right inferior temporal gyrus and middle temporal gyrus in homozygous carriers of the rs5569 G-allele in children with ADHD after treatment with methylphenidate [19]. To our best knowledge, no study has examined whether *SLC6A2* polymorphisms interfere with intrinsic brain activity in individuals with ADHD, as measured by functional magnetic resonance imaging (fMRI) without explicit tasks, i.e., resting-state fMRI (RS-fMRI).

There is growing evidence for poor performance on visual memory and visual attention tasks in children with ADHD, including impairment in delayed matching to sample (DMS) [20, 21] and Rapid Visual Information Processing (RVIP) [7, 22]. For example, children with ADHD have longer mean latency of correct responses in DMS [21] and higher misses in RVIP [22] than typically developing controls (TDC). Previous studies have converged to show a crucial role of norepinephrine in visual memory [23] and visual attention [24]. Significant associations between RS-fMRI signals and the outside-the-scanner performance on the DMS [25] and RVIP [26] have been noted in neurotypical individuals. Taken together, examining the relationships between *SLC6A2*, intrinsic brain activity, visual memory, and visual attention may provide insight into the pathways from *SLC6A2* to ADHD.

In this context, we aimed to investigate the differential brain effects as a function of the ADHD-related *SLC6A2* rs36011 (T)/rs1566652 (G) haplotype [4] by examining ReHo and DC in children with ADHD and typically developing children (TDC). In addition, we explored the relationships between *SLC6A2*-modulated brain alterations, visual memory, and visual attention to identify the gene-brain-behavior relationships in children with ADHD.

Materials and methods

Participants

The original sample consisted of 111 eligible drug-naïve children, with DSM-IV ADHD diagnosis, and 125 TDC, aged 7–16. ADHD children were recruited from the Department of Psychiatry, National Taiwan University Hospital, Taipei, Taiwan, consecutively. We recruited TDC children from similar school districts of ADHD children. We interviewed all the participants and their parents to confirm the ADHD diagnosis and to exclude other psychiatric disorders by using the Chinese Kiddie epidemiologic version of the Schedule for Affective Disorders and Schizophrenia (K-SADS-E) interview. The level of ADHD symptoms was determined by parent reports on the Chinese version of the Swanson, Nolan, and Pelham, version IV scale (SNAP-IV) [27].

Participants with full-scale IQ (FIQ) <80, any psychiatric disorder except ADHD, systemic diseases, or neurological disorders were excluded from the study. The informed consent procedures were approved by the Research Ethics Committee (IRB ID: 200903062R; ClinicalTrials.gov number, NCT00916851) of the National Taiwan University Hospital, Taiwan before study implementation. Written informed consent was obtained from all the participants and their parents, prior to the performance of any protocol-specific procedure.

Measurements

ADHD symptoms severity

The first 18 items of the SNAP-IV, a 26-item scale, include Inattention (IA, Item 1–9) and Hyperactivity/Impulsivity (HI, Item 10–18) subscales, corresponding to the ADHD core symptoms according to the DSM-IV criteria [28]. Each item is rated on a 4-point Likert scale (0 = not at all, 1 = just a little, 2 = quite a bit, 3 = very much). The Chinese SNAP-IV Parent Form has good validity and reliability [27]. The severity of ADHD symptomatology is the sum scores of IA and HI subscales (Item 1–18).

Measures of visual memory and visual attention

DMS and RVIP of the Cambridge Neuropsychological Test Automated Battery (CANTAB) were used to assess visual memory and visual attention, respectively.

Delayed matching to sample

We used the DMS task to measure the participant's ability to remember a complex visuo-spatial stimulus in a paradigm of delayed recognition memory [29]. The center of the

screen shows a sample pattern for 4.5 s at the outset of each trial. The sample pattern remains on the screen at the simultaneous matching condition when four choice patterns appear. A delay of 0, 4, or 12 s is introduced between covering the sample pattern and showing the choice patterns at the delayed condition. The participant is required to touch one of the four choice patterns that exactly matches the sample pattern. The mean times of correct responses taken in simultaneous and delay tasks are reported.

Rapid visual information processing

The RVIP assesses the participant's sustained visual attention [30]. Digits (2 to 9) appeared one at a time (100 digits/min) in the center of the screen in a random order. Participants have to detect three target sequences (3–5–7, 2–4–6, 4–6–8) and respond using a press pad when they see the last number (7, 6, and 8, respectively). Two indices, including total hits (the occasions the participant correctly responds), and total misses (the occasions the participant fails to respond) are reported.

Genotyping

We designed the primers by using the GenePipe (<http://genepipe.ibms.sinica.edu.tw/seqtool/pages/getSeq.jsp>) for retrieving the flanking sequences of SNP in the platform of National Genotyping Center of Academia Sinica (<http://lims.ngc.sinica.edu.tw/service/>). We performed the genotyping of rs36011 and rs1566652 with the matrix-assisted laser desorption/ionization time of flight mass spectrometry (MALDI-TOF MS). By using polymerase chain reaction (PCR) in GeneAmp 9700 thermocycler, we amplified the DNA fragment encompassing the SNP site. Then shrimp alkaline phosphatase (SAP) neutralized the unincorporated deoxynucleotide triphosphate of the PCR reaction mixture. After SAP activity was inactivated, we added the probe, Thermo Sequenase (Amersham Pharmacia, Piscataway, NJ, USA), for primer extension. Different products of the extension were differentiated by mass through MALDI-TOF after amplification. The method of MALDI-TOF has been applied in the genetic studies on ADHD [4, 31, 32] as it fulfilled criteria such as accuracy in detecting SNP, sensitivity to score SNPs, and cost-effectiveness.

Magnetic Resonance Imaging (MRI)

Data acquisition

By using a 32-channel phased-arrayed head coil, we obtained the MRI data on a 3T scanner (Siemens Magnetom Tim Trio). To complete a 6-min resting-state functional MRI (RS-fMRI) scan, all participants were verbally instructed to close their

eyes and remain still. We checked their prompt responses to technicians' questions to ensure wakefulness at the end of each scan. All participants denied that they had fallen into sleep during RS-fMRI scanning. The RS-fMRI parameters of echo planar imaging (EPI) were 180 volumes; repetition time (TR) = 2000 ms; echo time (TE) = 24 ms; flip angle = 90°; field of view (FOV) = 256 × 256 mm²; matrix size = 64 × 64; 34 axial slices acquired in an interleaved descending order; slice thickness = 3 mm; voxel size = 4 × 4 × 3 mm³; imaging plane being parallel to the anterior commissure-posterior commissure image plane. In addition, high-resolution T1-weighted images were acquired (MPRAGE, TR = 2000 ms; TE = 2.98 ms; inversion time (TI) = 900 ms; flip angle = 9°; FOV = 256 × 256 mm²; matrix size = 256 × 256 × 192; voxel size = 1 mm³ isotropic).

RS-fMRI data preprocessing

Standard resting-state EPI preprocessing was performed by employing the Data Processing Assistant for Resting-State fMRI (DPARSF) toolbox [33]. We discarded the first five EPI volumes of the scanning sessions to allow for signal equilibration. For each participant, functional images were slice time corrected. We realigned each volume to the first image volume with a six-parameter spatial transformation and a least-squares minimization. Realigned EPI images were registered to T1-weighted images, which were normalized to a Montreal Neurological Institute (MNI) template with isotropic 3 mm voxels through the gray matter (GM) segmentation obtained from structural images. We denoised the fMRI data by employing the Independent Component Analysis-based strategy for Automatic Removal of Motion Artifacts (ICA-AROMA) [34]. After motion denoising, we further denoised the EPI data by using the CONN toolbox v.15c [35] to remove other non-neuronal resources of noises with a component-based (anatomical CompCor) approach [36]. We included the first three principal components of the signals from the cerebral spinal fluid (CSF) and white matter (WM) ROIs, and linear detrending as regressors in the first-level regression model for denoising. Before performing the denoising regression, we filtered all of the regressors. Then the time course was temporally band-pass filtered (0.01–0.1 Hz), and linear drifts were removed.

Head motion

We estimated the in-scanner head motion by mean frame-wise displacement (FD) based on the measures derived from Jenkinson's algorithm of relative root mean square. We excluded participants with mean FD exceeding 1 standard deviation (SD, 0.14 mm) above the sample mean (0.19 mm) from further imaging analysis. As a result, 15 participants

with ADHD and 11 TDC were excluded, yielding a final sample of 210 participants.

ReHo analyses

We generated the ReHo map of each participant by computing the Kendall coefficient of concordance (KCC) of the time series of a given voxel with those of its nearest neighbors (26 voxels). We then adopted a whole-brain mask for removing the non-brain tissues. We divided the individual ReHo maps by their own global mean KCC within the whole-brain mask for standardization purposes. The generated ReHo maps were spatially smoothed with a Gaussian kernel of 4.5 mm full-width at half-maximum (FWHM).

DC analyses

We calculated the Pearson correlations between the time series of all pairs of brain voxels to obtain a whole-brain functional connectivity matrix for each participant. We obtained an undirected adjacency matrix by setting at Pearson's correlation at >0.25 level as the threshold for each correlation to eliminate counting voxels with a low-temporal correlation. For each voxel, a map of the degree was computed by counting the number of voxels to which it was connected. For standardization purposes, the individual-level voxel-wise DC value was converted to a DC Z-score map with Fisher's Z-transformation. The generated DC maps were spatially smoothed with a Gaussian kernel of 4.5 mm full-width at half-maximum (FWHM).

Statistical analyses

For baseline assessments of demographic data, we used percentage for categorical variables and mean scores and SD for continuous variables. According to the presence of the rs36011 (T)/rs1566652 (G) haplotype, we divided the genotypes of the *SLC6A2* variant into two groups: the TG group (TG haplotype carriers) and the Non-TG group (TG haplotype non-carriers). To examine the effects of ADHD and the *SLC6A2* TG haplotype on the ReHo and DC maps, a two-way ANOVA was performed with the factors diagnostic status (ADHD, TDC) and haplotype (TG, Non-TG) based on the full factorial design in SPM12. Age, sex, FIQ, and individual mean FD were included as nuisance covariates. To control for the false-positive error, we corrected all significant clusters at the cluster level by controlling topological family-wise error (FWE) computed according to Gaussian Random Field theory, employing a cluster-forming voxel-level height threshold of $p < 0.005$ and a spatial extent threshold ensuring a cluster-wise FWE at $p < 0.05$. We generated the group-wise GM mask, including voxels, which were present in all the participants. Because

of the finite spatial coverage of the EPI scan, the cerebellum was excluded from the resting imaging analyses.

To examine the relationship between *SLC6A2*-modulated intrinsic brain activity and neuropsychological functioning, those clusters showing significant effects of the TG haplotype in the ADHD group or diagnosis \times TG haplotype interaction were identified as ROIs. We then extracted the mean ReHo and DC values of these ROIs for partial correlation with the measures of DMS and RVIP, adjusting for age, sex, FIQ, and mean FD. To control for Type I error in correlation analyses, a false discovery rate (FDR) correction was set at $q < 0.05$.

Results

Demographic and clinical characteristics

These 210 participants were classified as either carriers of the *SLC6A2* rs36011 (T)/rs1566652 (G) haplotype (TG, $n = 45$ in the ADHD group and $n = 57$ in the TDC group) or non-carriers of this TG haplotype (Non-TG, $n = 51$ in the ADHD group and $n = 57$ in the TDC group). Supplementary Table 1 showed that each of the genotypes for rs36011 and rs1566652 fitted the values expected based on the Hardy–Weinberg equilibrium ($p > 0.05$). The distribution of the genetic variants in *SLC6A2* did not differ significantly between children with ADHD and TDC. Table 1 demonstrates that males were more predominant in the ADHD group than TDC. In addition, children with ADHD were younger and had lower FIQ, lower total hits, and higher total misses in RVIP than TDC. The TG carriers had higher HI scores than those without the TG haplotype.

Effects of ADHD on ReHo and DC

Compared with TDC, children with ADHD showed decreased ReHo in bilateral cuneus and lingual gyri (Table 2 and Fig. 1a) and decreased DC in the left cuneus and lingual gyrus (Table 2 and Fig. 1b).

Effects of TG haplotype on ReHo and DC

Compared with the non-carriers, the TG carriers showed significantly increased DC in the right precentral and postcentral gyri (Table 2 and Fig. 2a). Compared with ADHD children without the TG haplotype, ADHD children with the TG haplotype showed significantly increased ReHo and DC in bilateral precentral and postcentral gyri (Table 2 and Fig. 2b, c, respectively). To further disambiguate the refined effect of the TG haplotype on DC of the right precentral-postcentral cluster, the supplementary analysis was conducted excluding the participants with one TG

Table 1 Demographics, ADHD symptomatology, and performance on visual memory and visual attention between the four groups

	ADHD_TG (<i>n</i> = 45)	ADHD_NonTG (<i>n</i> = 51)	TDC_TG (<i>n</i> = 57)	TDC_NonTG (<i>n</i> = 57)	Diagnosis F or χ^2 (<i>p</i>)	Haplotype F or χ^2 (<i>p</i>)	Diagnosis by haplotype F (<i>p</i>)
Age							
Mean (SD)	11.2 (2.1)	11.8 (2.5)	12.4 (3.0)	12.3 (2.7)	5.89 (0.016)*	0.41 (0.52)	0.72 (0.4)
Sex							
Male (%)	37 (82.2)	45 (88.2)	39 (68.4)	35 (61.4)	11.47 (<0.001)***	0.005 (0.94)	
Handedness							
Right (%)	42 (93.3)	47 (92.2)	54 (94.7)	54 (94.7)	0.37 (0.54)	0.032 (0.86)	
FD							
Mean (SD)	0.14 (0.07)	0.16 (0.07)	0.13 (0.06)	0.14 (0.07)	3 (0.09)	1.7 (0.19)	0.9 (0.34)
FIQ							
Mean (SD)	106.9 (10.7)	102.5 (13.7)	108.9 (12.4)	111.3 (12.1)	10.1 (0.002)**	0.35 (0.56)	4.0 (0.05)
SNAP-IV							
Total ADHD scores	24.2 (11.3)	22.2 (8.7)	7.9 (7.6)	7.5 (6.8)	152.6 (<0.001)***	0.97 (0.32)	0.36 (0.55)
IA	13.7 (5.8)	14.2 (5.5)	4.4 (4.3)	4.4 (4.1)	174.6 (<0.001)***	0.13 (0.72)	0.1 (0.75)
HI	10.5 (6.3)	8 (5.3)	3.6 (3.9)	3.1 (3.6)	71.9 (<0.001)***	4.5 (0.035)*	2 (0.16)
DMS ^a							
Mean latency of correct responses (ms)							
Delay	3597 (952)	3461 (828)	3608 (1034)	3353 (875)	0.06 (0.8)	2.13 (0.17)	0.42 (0.52)
Simultaneous	3247 (928)	3143 (802)	3111 (1018)	2976 (1021)	0.01 (0.94)	0.54 (0.46)	0.05 (0.82)
RVP ^a							
Total hits	11.9 (4.3)	12.1 (5.6)	14.3 (5.4)	15 (5.3)	4.5 (0.04)*	0.3 (0.58)	0.4 (0.53)
Total misses	15.1 (4.3)	14.9 (5.5)	12.7 (5.4)	12 (5.3)	4.6 (0.03)*	0.3 (0.58)	0.36 (0.55)

ADHD attention-deficit hyperactivity disorder, TDC typically developing controls, FD frame-wise displacement, FIQ full intelligence quotient, SNAP-IV the Swanson, Nolan, and Pelham, version IV scale; IA inattention subscale, HI hyperactivity/Impulsivity subscale, DMS delayed matching to sample, RVP rapid visual information processing

* $p < 0.05$, ** $p < 0.01$, *** $p < 0.001$

^aControlled for age, sex, and FIQ

haplotype and other genetic variant (heterozygotes). Compared with the non-carriers, the homozygotes of the TG haplotype still demonstrated a significant increase in DC ($p = 0.02$) in the right precentral and postcentral gyri (Supplementary Table 2; detailed in Supplementary Information).

Effects of diagnosis \times TG haplotype interaction on ReHo and DC

Significant diagnosis by TG haplotype interactions were found in the right postcentral gyrus and superior parietal lobule for ReHo (Table 2 and Fig. 3a). In the ADHD group, ReHo in the right postcentral gyrus and superior parietal lobule increased with the TG haplotype (Fig. 3b), while in the TDC group, the reverse pattern was found.

Correlations between visual memory, visual attention, and SLC6A2-modulated differences in ReHo and DC

Previous studies have found that precentral gyrus [37, 38], postcentral gyrus [39, 40], and superior parietal lobule [41, 42] were involved in the information processing for visuo-spatial stimuli and played a crucial role in visual

memory and visual attention. Average ReHo and DC values were hence extracted from the four clusters showing significant effects of the TG haplotype in the ADHD group (bilateral precentral-postcentral gyri in ReHo and DC, respectively) or diagnosis \times TG haplotype interaction (the right postcentral gyrus-superior parietal lobule in ReHo) to calculate brain-behavior correlations. For the ADHD-TG group (Supplementary Table 3), there were positive correlations of mean latency of correct responses in the simultaneous tasks of the DMS with the ReHo of bilateral precentral-postcentral gyri ($r = 0.42$, $q = 0.024$); positive correlations of mean latency of correct responses in the simultaneous ($r = 0.4$, $q = 0.036$) and delay ($r = 0.37$, $q = 0.04$) tasks of the DMS with the ReHo of the right postcentral gyrus-superior parietal lobule; and negative correlations of total hits ($r = -0.36$, $q = 0.04$) and positive correlations of total misses ($r = 0.36$, $q = 0.04$) in RVP with the DC of the left precentral-postcentral gyri.

Effects of HI and HI \times TG haplotype interaction on DMS, RVP, and DC

Since carriers with the TG haplotype showed higher levels of hyperactivity in both ADHD and TDC groups, we divided all the subjects based on the severity of HI scores

Table 2 Significant clusters with the effects of ADHD and the TG haplotype on ReHo and DC

Area	ReHo					DC				
	Hemisphere	Volume (mm ³)	MNI coordinates ^a	T value ^a	Area	Hemisphere	Volume (mm ³)	MNI coordinates ^a	T value ^a	
			x	y	z			x	y	z
ADHD effect (ADHD vs. neurotypical)										
Cuneus-lingual gyrus (VIS)	B	7182	0	-66	3	L	3132	3	-57	6
TG haplotype effect (TG vs. Non-TG)										
ADHD-TG vs. ADHD-Non-TG										
Precentral-postcentral gyri (SSM)	B	11961	-3	-30	72	L	4185	-57	-12	45
						R	5292	36	-33	54
Diagnosis × TG haplotype										
Postcentral gyrus- superior parietal lobule (SSM and DAN)	R	6480	9	-39	72					
ADHD attention-deficit hyperactivity disorder, DC degree centrality, ReHo regional homogeneity, L left, R right, B bilateral, VIS visual network, SSM somatosensory and motor network, DAN dorsal attention network										
^a Based on the peak voxel										

rather than diagnosis in order to examine the brain and behavioral effects of HI and HI × haplotype interaction. Our findings showed that there were no significant effects of HI or HI × TG haplotype interaction on the DMS, RVIP, and DC in the right precentral-postcentral gyri (Supplementary Table 4; detailed in Supplementary Information). We further used the original diagnostic group classification, but controlled for dimensional HI score, in addition to the aforementioned nuisance covariates in the model. In this supplementary analysis additionally covarying HI levels, the TG carriers still showed a significant increase in DC ($p = 0.001$) in the right precentral and postcentral gyri (Supplementary Table 5).

Discussion

This study is the first to demonstrate that ReHo and DC in sensorimotor and dorsal attention networks are modulated by the *SLC6A2* rs36011 (T)/rs1566652 (G) haplotype in children with ADHD, and also the first to demonstrate that these *SLC6A2*-modulated alterations in ReHo and DC are related to visual memory and visual attention. Our findings provide evidence that the *SLC6A2* rs36011 (T)/rs1566652 (G) haplotype may play an important role in altered intrinsic brain activity, visual memory, and visual attention in children with ADHD.

Regardless of *SLC6A2* genotypes, we identify reduced ReHo in bilateral cuneus and lingual gyri, and reduced DC in the left cuneus and lingual gyrus in children with ADHD. Previous studies have shown that neurobiological alterations of cuneus [13, 43], and lingual gyrus [44] are implicated in the pathophysiology of ADHD. These brain regions are also functionally involved in neuropsychological difficulties associated with ADHD, especially during working memory processing [43] and task switching [44].

Our present study demonstrated differential intrinsic brain activity related to the *SLC6A2* rs36011 (T)/rs1566652 (G) in the sensorimotor network. Compared with the ADHD-Non-TG group, the ADHD-TG group showed increased ReHo and DC in bilateral precentral and postcentral gyri. Previous studies have documented the involvement of the sensorimotor network in the pathogenesis of ADHD [45, 46]. In addition, norepinephrine and NET play a crucial role in the functions of the sensorimotor network [47]. Activation of motor cortex for response inhibition in youths with ADHD has been found to predict clinical response to atomoxetine [48], a selective inhibitor of NET. Our previous work shows that after 12 weeks of treatment with atomoxetine, the improvement in the scores of hyperactivity/impulsivity correlates with decreased intrinsic brain activity in bilateral precentral and postcentral gyri in patients with ADHD [49]. Our present study extends these

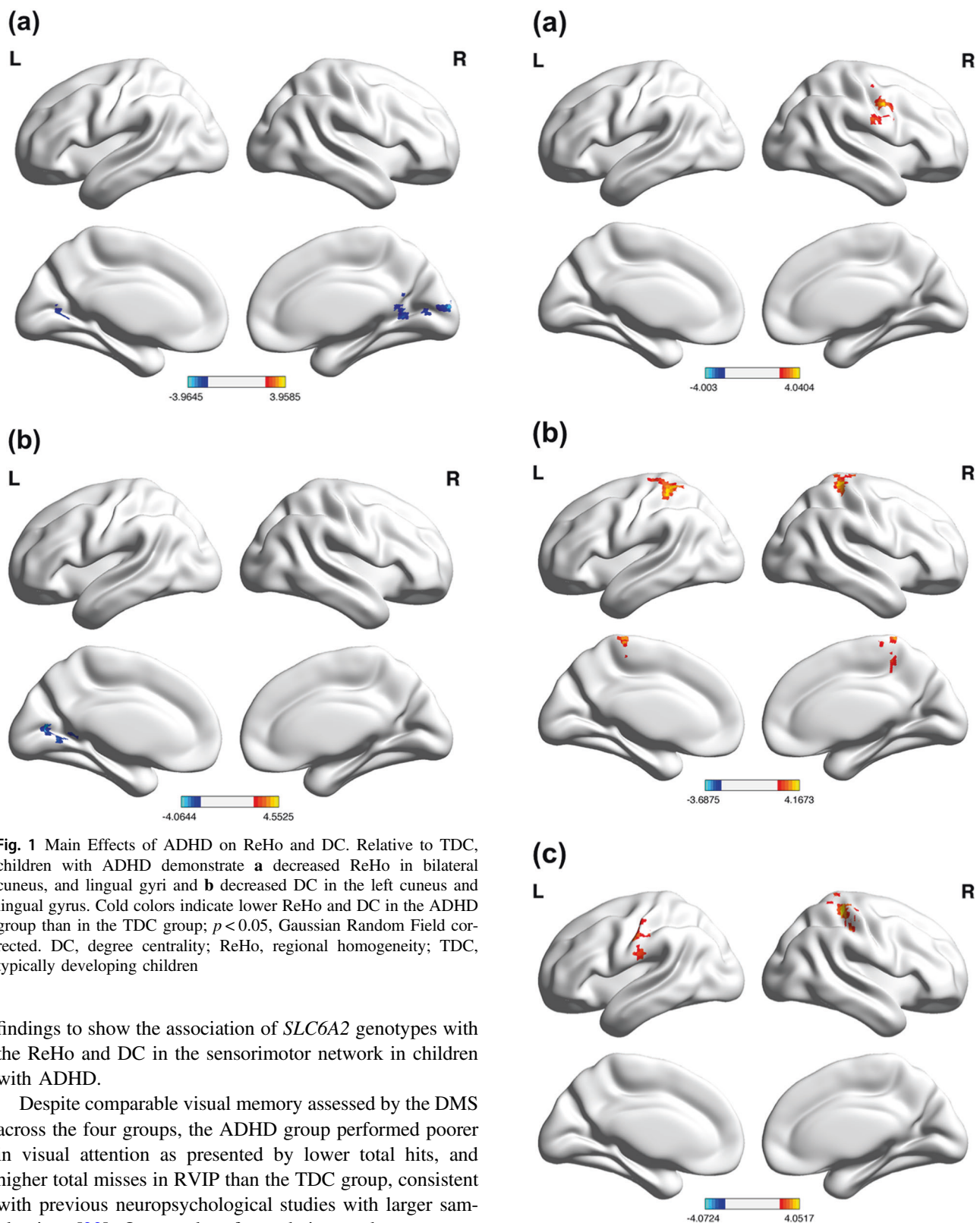


Fig. 1 Main Effects of ADHD on ReHo and DC. Relative to TDC, children with ADHD demonstrate **a** decreased ReHo in bilateral cuneus, and lingual gyri and **b** decreased DC in the left cuneus and lingual gyrus. Cold colors indicate lower ReHo and DC in the ADHD group than in the TDC group; $p < 0.05$, Gaussian Random Field corrected. DC, degree centrality; ReHo, regional homogeneity; TDC, typically developing children

findings to show the association of *SLC6A2* genotypes with the ReHo and DC in the sensorimotor network in children with ADHD.

Despite comparable visual memory assessed by the DMS across the four groups, the ADHD group performed poorer in visual attention as presented by lower total hits, and higher total misses in RVIP than the TDC group, consistent with previous neuropsychological studies with larger sample sizes [22]. Our results of correlation analyses suggest that increased ReHo and DC in the sensorimotor network are associated with a slower reaction time of visual memory and decreased the accuracy of visual attention in the ADHD-TG group. Animal studies demonstrate that neurons

in the somatosensory cortex are activated during the DMS task [50]. In addition, the motor cortex is reported to be involved in performance on the RVIP task [51]. Our

Fig. 2 Main effects of the TG haplotype on ReHo and DC. Relative to participants without the TG haplotype, those with this haplotype demonstrate **a** increased DC in the right precentral and postcentral gyri. For the ADHD group, children with the TG haplotype show increased **b** ReHo and **c** DC in bilateral precentral and postcentral gyri. Hot colors indicate higher ReHo and DC in the TG group than in the non-TG group; $p < 0.05$, Gaussian Random Field corrected. DC, degree centrality; ReHo, regional homogeneity

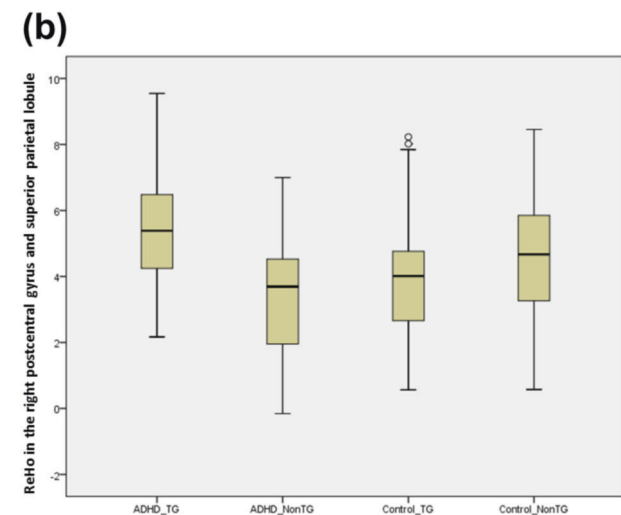
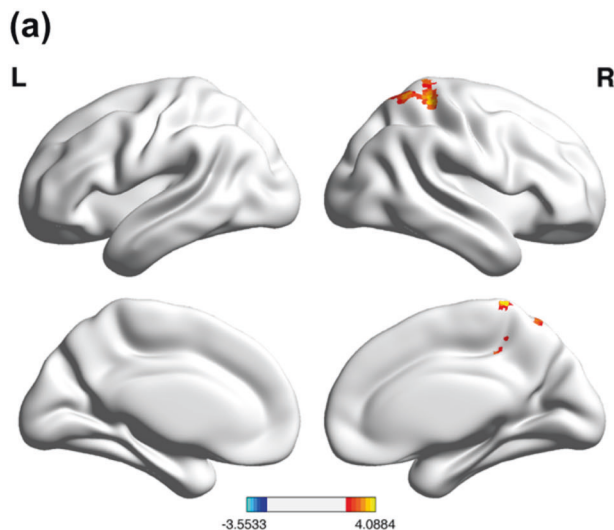


Fig. 3 Effects of interaction of diagnosis \times TG haplotype on ReHo. **a** Significant interactions are found in the right postcentral gyrus and superior parietal lobule. $p < 0.05$, Gaussian Random Field corrected. **b** Comparison of ReHo in the right postcentral gyrus and superior parietal lobule across the four groups using box and whisker plots. The box boundaries represent first and third quartiles, and the midline is the median. Dots represent values > 1.5 box lengths from the upper or lower edges. ReHo, regional homogeneity

findings imply that genetically determined differences in the sensorimotor network may contribute to the performance of the visual memory and visual attention tasks in ADHD children with the TG haplotype. Taken together, our results of gene-brain-behavior linkage within one study are

supported by existing literature describing norepinephrine-sensorimotor network [47, 48], sensorimotor network-visual memory and visual attention [50, 51], and norepinephrine-visual memory and visual attention [23, 24] relationships. Our findings may contribute to a model of visual memory and visual attention enabled by the norepinephrine-related sensorimotor network in children with ADHD.

A significant interaction between ADHD diagnosis and TG haplotype is observed in the right postcentral gyrus-superior parietal lobule on ReHo, with the ADHD-TG group having the greatest ReHo among the four groups. Previous studies demonstrate an abnormality in the parietal regions associated with the dorsal attentional network in ADHD [52], and the superior parietal lobule plays a crucial role in visual memory in youths with ADHD [53]. After treatment with methylphenidate, ReHo in the right postcentral gyrus-superior parietal lobule decreases significantly in children with ADHD [12]. The present study extends these findings to show that the *SLC6A2*-related ReHo alterations in the superior parietal lobule may be associated with the visual memory performance in children with ADHD.

Methodological considerations

Several methodological limitations have to be considered while interpreting our results. First, due to the referred sample with strict inclusion and exclusion criteria, our results may not be generalized to the community-based ADHD population. Second, the structural architecture and functional organization of the human brain undergo significant changes across the life span [54]. Given that ADHD is associated with a delay in cortical maturation [55], and brain alterations change with developmental stages in patients with ADHD [56], group differences observed in cross-sectional neuroimaging studies may vary according to the age range of the sample examined. Although we include age as a covariate in analyses, a wide age range of participants may potentially confound our findings with multiple stages of brain development. Third, we acknowledge that the present genetic-imaging-behavioral approach in a cross-sectional cohort is observational and correlational, and further research with additional levels and novel integration of methodologies are needed to investigate the functional effects of the *SLC6A2* rs36011 (T)/rs1566652 (G) haplotype in children with ADHD. Fourth, although previous studies have shown significant associations between RS-fMRI data and the performance on the DMS [25] and RVIP [26] tasks outside the MRI scanner, this approach could potentially weaken the link between RS-fMRI data and neuropsychological performance by time effects. Future studies based on fMRI evoked by visual memory and visual attention tasks are required to replicate the current findings. However, it might also suggest that the observed associations of

alterations in ReHo and DC with visual memory and visual attention are more likely to reflect trait-like features rather than state contingencies. Fifth, given that the sample size with two TG haplotypes is small (nine in the ADHD-TG group and ten in the TDC-TG group), future imaging genetics investigations are warranted to explore the differential behavioral and brain effects between the homozygous and heterozygous carriers of the TG haplotype in a larger sample.

In conclusion, we provide the first empirical data to suggest genotypes of the norepinephrine transporter gene modulate local intrinsic brain activity of the sensorimotor and dorsal attention networks in ADHD. Moreover, visual memory and attention performances of ADHD are influenced by these gene-brain modulations. These findings advance our understanding of genetic underpinnings of neurobiological abnormalities in children with ADHD and provide insight into the underlying neurochemical modulation of ReHo and DC.

Acknowledgements This study was supported by grants NSC96-2628-B-002-069-MY3, NSC98-2314-B-002-051 -MY3, NSC99-2321-B-002-037, and NSC101-2321-B-002-079 from Ministry of Science and Technology (Taiwan) and grants NHRI-EX98-9407PC and NHRI-EX100-0008PI from National Health Research Institute (Taiwan). SNP genotyping was performed by the National Genotyping Center of Academia Sinica, Taiwan, and by the support from the Department of Medical Research, National Taiwan University Hospital, Taipei, Taiwan.

Author contributions CYS and SSG contributed to concept and design of the study. CYS and SSG contributed to data acquisition. CYS, HYL, and SSG contributed to data analysis/interpretation. CYS contributed to drafting the manuscript, tables, and figures, which were critically reviewed by SSG. All authors read and approved the final version of the manuscript.

Compliance with ethical standards

Conflict of interest The authors declare that they have no conflict of interest.

Publisher's note Springer Nature remains neutral with regard to jurisdictional claims in published maps and institutional affiliations.

References

1. Arnsten AF. Fundamentals of attention-deficit/hyperactivity disorder: circuits and pathways. *J Clin Psychiatry* 2006;67(Suppl 8):7–12.
2. Carboni E, Silvagni A. Dopamine reuptake by norepinephrine neurons: exception or rule? *Crit Rev Neurobiol* 2004;16:121–8.
3. Bonisch H, Bruss M. The norepinephrine transporter in physiology and disease. *Handb Exp Pharmacol*. 2006;175:485–524.
4. Shang CY, Chiang HL, Gau SS. A haplotype of the norepinephrine transporter gene (SLC6A2) is associated with visual memory in attention-deficit/hyperactivity disorder. *Prog Neuropsychopharmacol Biol Psychiatry* 2015;58:89–96.
5. Bobb AJ, Addington AM, Sidransky E, Gornick MC, Lerch JP, Greenstein DK, et al. Support for association between ADHD and

- two candidate genes: NET1 and DRD1. *Am J Med Genet B Neuropsychiatr Genet* 2005;134B:67–72.
6. Klein M, Onnink M, van Donkelaar M, Wolfers T, Harich B, Shi Y, et al. Brain imaging genetics in ADHD and beyond - Mapping pathways from gene to disorder at different levels of complexity. *Neurosci Biobehav Rev* 2017;80:115–55.
7. Shang CY, Wu YH, Gau SS, Tseng WY. Disturbed microstructural integrity of the frontostriatal fiber pathways and executive dysfunction in children with attention deficit hyperactivity disorder. *Psychol Med*. 2013;43:1093–107.
8. Castellanos FX, Aoki Y. Intrinsic functional connectivity in attention-deficit/hyperactivity disorder: a science in development. *Biol Psychiatry Cogn Neurosci Neuroimaging* 2016;1:253–61.
9. Zang Y, Jiang T, Lu Y, He Y, Tian L. Regional homogeneity approach to fMRI data analysis. *Neuroimage* 2004;22:394–400.
10. Zuo XN, Ehmke R, Mennes M, Imperati D, Castellanos FX, Sporns O, et al. Network centrality in the human functional connectome. *Cereb Cortex* 2012;22:1862–75.
11. Cheng W, Ji X, Zhang J, Feng J. Individual classification of ADHD patients by integrating multiscale neuroimaging markers and advanced pattern recognition techniques. *Front Syst Neurosci* 2012;6:58.
12. An L, Cao XH, Cao QJ, Sun L, Yang L, Zou QH, et al. Methylphenidate normalizes resting-state brain dysfunction in boys with attention deficit hyperactivity disorder. *Neuropsychopharmacology*. 2013;38:1287–95.
13. Alonso Bde C, Hidalgo Tobon S, Dies Suarez P, Garcia Flores J, de Celis Carrillo B, Barragan Perez E. A multi-methodological MR resting state network analysis to assess the changes in brain physiology of children with ADHD. *PLoS ONE*. 2014;9:e99119.
14. Wang JB, Zheng LJ, Cao QJ, Wang YF, Sun L, Zang YF, et al. Inconsistency in abnormal brain activity across cohorts of ADHD-200 in children with attention deficit hyperactivity disorder. *Front Neurosci* 2017;11:320.
15. Wang X, Jiao Y, Tang T, Wang H, Lu Z. Altered regional homogeneity patterns in adults with attention-deficit hyperactivity disorder. *Eur J Radio*. 2013;82:1552–7.
16. Di Martino A, Zuo XN, Kelly C, Grzadzinski R, Mennes M, Schvarcz A, et al. Shared and distinct intrinsic functional network centrality in autism and attention-deficit/hyperactivity disorder. *Biol Psychiatry*. 2013;74:623–32.
17. Wu Z, Yang L, Wang Y. Applying imaging genetics to ADHD: the promises and the challenges. *Mol Neurobiol* 2014;50:449–62.
18. Sigurdardottir HL, Kranz GS, Rami-Mark C, James GM, Vanicek T, Gryglewski G, et al. Effects of norepinephrine transporter gene variants on NET binding in ADHD and healthy controls investigated by PET. *Hum Brain Mapp* 2016;37:884–95.
19. Park MH, Kim JW, Yang YH, Hong SB, Park S, Kang H, et al. Regional brain perfusion before and after treatment with methylphenidate may be associated with the G1287A polymorphism of the norepinephrine transporter gene in children with attention-deficit/hyperactivity disorder. *Neurosci Lett*. 2012;514:159–63.
20. Barnett R, Maruff P, Vance A. Neurocognitive function in attention-deficit-hyperactivity disorder with and without comorbid disruptive behaviour disorders. *Aust N Z J Psychiatry* 2009;43:722–30.
21. Shang CY, Gau SS. Visual memory as a potential cognitive endophenotype of attention deficit hyperactivity disorder. *Psychol Med*. 2011;41:2603–14.
22. Gau SS, Huang WL. Rapid visual information processing as a cognitive endophenotype of attention deficit hyperactivity disorder. *Psychol Med*. 2014;44:435–46.
23. Moor T, Mundorff L, Bohringer A, Philippsen C, Langewitz W, Reino ST, et al. Evidence that baroreflex feedback influences long-term incidental visual memory in men. *Neurobiol Learn Mem* 2005;84:168–74.

24. Gau SS, Shang CY. Improvement of executive functions in boys with attention deficit hyperactivity disorder: an open-label follow-up study with once-daily atomoxetine. *Int J Neuropsychopharmacol* 2010;13:243–56.
25. Grady CL, Protzner AB, Kovacevic N, Strother SC, Afshin-Pour B, Wojtowicz M, et al. A multivariate analysis of age-related differences in default mode and task-positive networks across multiple cognitive domains. *Cereb Cortex* 2010;20:1432–47.
26. Pagnoni G. Dynamical properties of BOLD activity from the ventral posteromedial cortex associated with meditation and attentional skills. *J Neurosci*. 2012;32:5242–49.
27. Gau SS, Shang CY, Liu SK, Lin CH, Swanson JM, Liu YC, et al. Psychometric properties of the Chinese version of the Swanson, Nolan, and Pelham, version IV scale - parent form. *Int J Methods Psychiatr Res* 2008;17:35–44.
28. Swanson JM, Kraemer HC, Hinshaw SP, Arnold LE, Conners CK, Abikoff HB, et al. Clinical relevance of the primary findings of the MTA: success rates based on severity of ADHD and ODD symptoms at the end of treatment. *J Am Acad Child Adolesc Psychiatry* 2001;40:168–79.
29. Egerhazi A, Berecz R, Bartok E, Degrell I. Automated Neuropsychological Test Battery (CANTAB) in mild cognitive impairment and in Alzheimer's disease. *Prog Neuropsychopharmacol Biol Psychiatry* 2007;31:746–51.
30. Sahakian B, Jones G, Levy R, Gray J, Warburton D. The effects of nicotine on attention, information processing, and short-term memory in patients with dementia of the Alzheimer type. *Br J Psychiatry* 1989;154:797–800.
31. Shang CY, Gau SS. Association between the DAT1 gene and spatial working memory in attention deficit hyperactivity disorder. *Int J Neuropsychopharmacol* 2014;17:9–21.
32. Shang CY, Gau SS, Liu CM, Hwu HG. Association between the dopamine transporter gene and the inattentive subtype of attention deficit hyperactivity disorder in Taiwan. *Prog Neuropsychopharmacol Biol Psychiatry* 2011;35:421–8.
33. Yan CG, Zang YF. DPARSF: A MATLAB toolbox for “pipeline” data analysis of resting-state fMRI. *Front Syst Neurosci*. 2010;4:13.
34. Pruim RH, Mennes M, Buitelaar JK, Beckmann CF. Evaluation of ICA-AROMA and alternative strategies for motion artifact removal in resting state fMRI. *Neuroimage* 2015;112:278–87.
35. Whitfield-Gabrieli S, Nieto-Castanon A. Conn: a functional connectivity toolbox for correlated and anticorrelated brain networks. *Brain Connect* 2012;2:125–41.
36. Behzadi Y, Restom K, Liu J, Liu TT. A component based noise correction method (CompCor) for BOLD and perfusion based fMRI. *NeuroImage* 2007;37:90–101.
37. Hahn B, Ross TJ, Stein EA. Neuroanatomical dissociation between bottom-up and top-down processes of visuospatial selective attention. *Neuroimage* 2006;32:842–53.
38. Huettel SA, Guzelcure G, McCarthy G. Dissociating the neural mechanisms of visual attention in change detection using functional MRI. *J Cogn Neurosci* 2001;13:1006–18.
39. Balslev D, Odoj B, Karnath HO. Role of somatosensory cortex in visuospatial attention. *J Neurosci*. 2013;33:18311–8.
40. Suchan B, Botko R, Gizewski E, Forsting M, Daum I. Neural substrates of manipulation in visuospatial working memory. *Neuroscience* 2006;139:351–7.
41. Bueicheku E, Ventura-Campos N, Palomar-Garcia MA, Miro-Padilla A, Parcet MA, Avila C. Functional connectivity between superior parietal lobule and primary visual cortex “at rest” predicts visual search efficiency. *Brain Connect* 2015;5:517–26.
42. Koenigs M, Barbey AK, Postle BR, Grafman J. Superior parietal cortex is critical for the manipulation of information in working memory. *J Neurosci*. 2009;29:14980–6.
43. Wolf RC, Plichta MM, Sambataro F, Fallgatter AJ, Jacob C, Lesch KP, et al. Regional brain activation changes and abnormal functional connectivity of the ventrolateral prefrontal cortex during working memory processing in adults with attention-deficit/hyperactivity disorder. *Hum Brain Mapp* 2009;30:2252–66.
44. Dibbets P, Evers EA, Hurks PP, Bakker K, Jolles J. Differential brain activation patterns in adult attention-deficit hyperactivity disorder (ADHD) associated with task switching. *Neuropsychology* 2010;24:413–23.
45. Mostofsky SH, Rimrodt SL, Schafer JG, Boyce A, Goldberg MC, Pekar JJ, et al. Atypical motor and sensory cortex activation in attention-deficit/hyperactivity disorder: a functional magnetic resonance imaging study of simple sequential finger tapping. *Biol Psychiatry*. 2006;59:48–56.
46. Valera EM, Spencer RM, Zeffiro TA, Makris N, Spencer TJ, Faraone SV, et al. Neural substrates of impaired sensorimotor timing in adult attention-deficit/hyperactivity disorder. *Biol Psychiatry*. 2010;68:359–67.
47. Bekar LK, Wei HS, Nedergaard M. The locus coeruleus-norepinephrine network optimizes coupling of cerebral blood volume with oxygen demand. *J Cereb Blood Flow Metab* 2012;32:2135–45.
48. Schulz KP, Bedard AV, Fan J, Hildebrandt TB, Stein MA, Ivanov I, et al. Striatal activation predicts differential therapeutic responses to methylphenidate and atomoxetine. *J Am Acad Child Adolesc Psychiatry* 2017;56:602–9.
49. Shang CY, Yan CG, Lin HY, Tseng WY, Castellanos FX, Gau SS. Differential effects of methylphenidate and atomoxetine on intrinsic brain activity in children with attention deficit hyperactivity disorder. *Psychol Med*. 2016;46:3173–85.
50. Wang L, Li X, Hsiao SS, Bodner M, Lenz F, Zhou YD. Persistent neuronal firing in primary somatosensory cortex in the absence of working memory of trial-specific features of the sample stimuli in a haptic working memory task. *J Cogn Neurosci* 2012;24:664–76.
51. Coull JT, Frith CD, Frackowiak RS, Grasby PM. A fronto-parietal network for rapid visual information processing: a PET study of sustained attention and working memory. *Neuropsychologia* 1996;34:1085–95.
52. Castellanos FX, Proal E. Large-scale brain systems in ADHD: beyond the prefrontal-striatal model. *Trends Cogn Sci* 2012;16:17–26.
53. Fan LY, Gau SS, Chou TL. Neural correlates of inhibitory control and visual processing in youths with attention deficit hyperactivity disorder: a counting Stroop functional MRI study. *Psychol Med*. 2014;44:2661–71.
54. Casey BJ, Tottenham N, Liston C, Durston S. Imaging the developing brain: what have we learned about cognitive development? *Trends Cogn Sci* 2005;9:104–10.
55. Shaw P, Malek M, Watson B, Sharp W, Evans A, Greenstein D. Development of cortical surface area and gyrification in attention-deficit/hyperactivity disorder. *Biol Psychiatry*. 2012;72:191–7.
56. Frodl T, Skokauskas N. Meta-analysis of structural MRI studies in children and adults with attention deficit hyperactivity disorder indicates treatment effects. *Acta Psychiatr Scand*. 2012;125:114–26.